Grid travel–time tracing: second–order method for the first arrivals in smooth media

Luděk Klimeš

Department of Geophysics, Charles University, Ke Karlovu 3, 121 16 Praha 2, Czech Republic, E-mail: klimes@seis.karlov.mff.cuni.cz

Abstract

A new computational scheme for calculating the first–arrival travel times on a rectangular grid of points is proposed. The new proposed method is of second–order accuracy. This means that the error of the calculated travel time is proportional to the second power of the grid spacing. The method should be sufficiently accurate for all applications in smooth seismic models. On the other hand, the method is not, in its present form, proposed for models with structural interfaces which make the method unstable and generate travel–time errors of the first order. Equations are also presented for the appropriate evaluation of the errors of calculated travel times to check their accuracy, and the proposed method is compared with other numerical methods. The method is developed, described, and demonstrated in 2-D, but may also be extended to 3-D models and to general models with structural interfaces.

Keywords

Seismic waves, first–arrival travel times, slowness vectors, ray tracing, accuracy.

1 Introduction

In recent years, many authors have proposed methods of calculating travel times on regular rectangular grids of points. The grids represent discretized forms of seismic models, as in full–wave finite–difference methods. The error of calculated travel time is then proportional to some power of the grid spacing. The *accuracy order* of the numerical method refers to this power. As a rule, the *grid* travel–time calculating methods have been proposed for *first–arrival travel times*, and may be divided into two classes:

(a) Methods interpolating already calculated travel times between gridpoints in order to evaluate the travel time at the closest next gridpoint. These methods are often called "finite–difference" eikonal–equation solvers, but the author would prefer some other common name, for instance *grid travel–time tracing* proposed here, because the ordinary meaning of "finite–differences" would have to be generalized considerably to include all these methods as well. These methods developed from the noncausal (but second–order in a smooth medium) method of Vidale (1988), through its causal modification by Qin et al. (1990, 1992) and many other algorithms, to the stable but first–order method of Podvin and Lecomte (1991). The accuracy of the first–order methods may be increased considerably by replacing the plane wavefront approximation with a method of higher order, if the updating scheme is made stable for the interpolation method. The accuracy of the second–order methods may be increased considerably by local application of spherical wavefronts (not by using general spherical coordinates centred at the point source) and by accurate travel–time matching at structural interfaces.

Pure appl. Geophys., 148 (1996), 539–563.

(b) Methods based on shortest–path network algorithms. They developed from the less accurate methods of orders between 0 and $2/3$ by Nakanishi and Yamaguchi (1986), Moser (1989, 1991), and Saito (1989, 1990), to the self–adaptable algorithm of the first order by Klimeš and Kvasnička (1994).

Note that many other methods of travel–time calculation, not connected with regular rectangular grids of points and mostly devoted to *ray–theory* (instead of first–arrival) *travel times*, like wavefront tracing by Vinje, Iversen and Gjøystdal (1993) for example, are not discussed here.

The method proposed here follows the grid travel–time tracing approach (a), and is based on the idea of calculating the *slowness vectors* at gridpoints together with *travel times*. The simultaneous calculation of the slowness vectors and travel times has already been proposed by Van Trier and Symes (1990, 1991). Pusey and Vidale (1991) then applied centred differences to the slowness–vector components and obtained the very accurate second–order method for smooth media.

In the method proposed here, the travel times between two adjacent gridpoints are interpolated by an accurate second–order or third–order method. The point on the gridline segment, from which the ray propagates to the next gridpoint, is approximated with an accuracy proportional to the square of the grid spacing. Slowness is interpolated linearly. From the point on the gridline segment, the slowness vectors and travel times are approximated by expansions accurate up to terms with second partial travel–time derivatives. Thus, in a smooth medium, the resulting travel–time error corresponds to the neglected second partial slowness derivatives, and is of the order of the squared grid interval. The rays are then approximated very accurately in the smooth parts of the model, i.e. in the regions where the second partial slowness derivatives are kept within some reasonable finite limits. This is not the case of the first– and second–order interfaces, where the method has to be generalized by means of matching travel times on both sides of the interface.

The method is briefly explained in Section 2. The equations for the extrapolation of the first–arrival travel times and the corresponding slowness vectors to the next gridpoint are given in Section 3. The relative first–arrival travel–time error of the proposed 2-D second–order method is estimated in Section 4. To compare the proposed method with two first–order methods, the relative travel–time error estimation of network ray tracing by Klimeš and Kvasnička (1994) is specified for 2-D smooth models in Section 5.1, and the relative travel–time error of the first–order method by Podvin and Lecomte (1991) in 2-D smooth models is estimated in Section 5.2. The accuracy estimation of Section 5.2 may also be used as a stand–alone result by people using the programs based on the algorithm by Podvin and Lecomte (1991). Theoretical accuracy estimations of Sections 4 and 5 are illustrated by simple numerical examples in Section 6.

2 Algorithm

Slowness vectors are calculated at gridpoints together with *travel times*. This means that, in 2-D, instead of each slowness describing the discretized smooth model, 2 components of the slowness vector have to be stored in memory. The length of the slowness vector is, of course, equal to the slowness and is not changed during the calculation. Before calculation, input velocities are transformed to slowness vectors of arbitrary orientation. During the updating process, the orientations of the slowness vectors are corrected step–by–step, without changing their lengths.

Thus, in 2-D smooth models, 4 storage locations are required per one gridpoint: 1 travel time, 2 components of the slowness vector, and 1 index in the *waiting queue*. This queue contains the indices of the gridpoints waiting to initiate updating of other gridpoints. A gridpoint may *initiate updating* of its neighbouring gridpoints if it is known that the gridpoint will not further be updated.

Updating of a gridpoint then consists in evaluating a new estimation of the minimum travel time at the gridpoint, i.e. in finding the minimum travel time corresponding to the considered kinds of travel–time propagation and updating the previous estimation of the minimum travel time. Under travel–time propagation we include here the considered ray paths leading to the gridpoint, at which the travel time is calculated, from the gridpoints or gridline segments where the travel time has already been determined.

Two different kinds of travel–time propagation are considered:
(**a**) the travel–time field interpolated along the gridline segment between two adjacent gridpoints and propagating along rays perpendicular to the local wavefronts, called *"refracted"* hereinafter.
(**b**) *diffractions at gridpoints.*

"Refracted" travel–time fields (**a**) are taken into account just in the region between two half–lines given by the slowness vectors. Only the end gridpoints of the two nearest parallel gridline segments may be updated. See Figure 1.

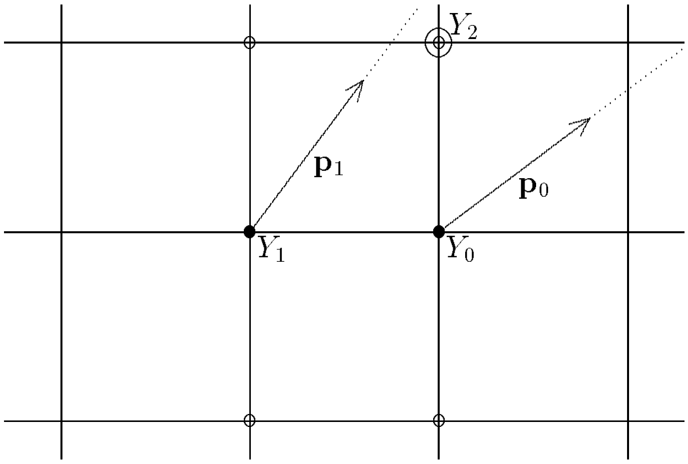

Figure 1. •'s denote two end gridpoints of the gridline segment along which the travel time has already been determined and which initiate updating; ∘'s denote the end gridpoints of the two nearest parallel gridline segments; ◯ denotes the gridpoint to be updated if the new travel time is less than the previously determined value.

Diffracted travel–time fields (**b**) are taken into account at all 8 nearest gridpoints.

Source. For the sake of conciseness, we consider only an arbitrarily positioned point source in this paper.

Initialization. When starting the algorithm, gridpoints surrounding the source are updated and put at the beginning of the queue. By the surrounding gridpoints we mean here all gridpoints situated in the square of half–side $(h+H)$ centred at the point source. Here H is a small positive length not exceeding the grid interval h in order of magnitude. For example, the author presently applies $H = \frac{1}{2}h$. Updating consists in determining the travel times and slowness vectors, and for the point source is, of course, of diffraction type (**b**) with diffraction at the point source.

There exists minimum travel–time increment $d_{\min}$, such that the travel time at the updated gridpoint Y_2 is at least by $d_{\min}$ greater than the travel time at the gridpoint initiating updating, see Section 2.1. We may thus separate the gridpoints, according to first–arrival travel times, into intervals of length not exceeding $d_{\min}$. The node being updated then belongs to a higher interval than nodes Y_0 and Y_1 initiating updating, and the `INTERVAL` algorithm by Klimeš and Kvasnička (1994) can be used to select the gridpoints to initiate the updating of the neighbouring gridpoints.

The `INTERVAL` *algorithm.* The gridpoints from the waiting queue are separated into *intervals* of lengths $d_{\min}$ according to their travel time. Instead of searching for the gridpoint of the minimum travel time, all gridpoints from the lowest nonempty interval may initiate updating. The updated nodes then belong to intervals higher than the lowest nonempty interval. That is why the gridpoints from the lowest nonempty interval cannot further be updated and may thus initiate updating. At the beginning, only the gridpoints with travel time determined during the initialization are stored in an unsorted queue. The queue may be represented, e.g., by an array Q in which the indices of the gridpoints are being stored. Once the gridpoint has been updated, it is added to the queue. First, updating is initiated by the nodes in the queue belonging to the lowest travel–time interval of size $d_{\min}$. The gridpoints which have already initiated updating are removed from the queue. Once all gridpoints of the interval are removed from the queue, we proceed to the next travel–time interval of length $d_{\min}$, and this procedure is repeated until the queue is empty.

Now the reader may have noticed that we have spoken of a single gridpoint initiating updating, whereas "refraction" travel–time propagation (**a**) is initiated by a couple of neighbouring gridpoints. If a gridpoint is selected by the `INTERVAL` algorithm to initiate updating, all 4 neighbouring nodes (in 2-D) are searched for travel times not exceeding the travel time at the selected gridpoint. The "refraction" updating (**a**) is then started from all gridline segments Y_0Y_1 connecting the gridpoint initiating updating with a gridpoint of less or equal travel time. There should be, in most cases but not always, 2 such gridlines per each gridpoint in 2-D.

Each gridline Y_0Y_1 may initiate updating of at most 2 of 4 end gridpoints of the nearest parallel gridline segments. There will be, in most cases but not always, 0 or 1 such points Y_2 per each gridline segment Y_0Y_1 in 2-D, one half on the average. Two points Y_2 per gridline segment Y_0Y_1 are not expected to be frequent in smooth models.

2.1 Minimum travel–time increment in 2-D

A locally homogeneous medium of the slowness equal to the minimum slowness $u_{\rm min}$ in the model will be assumed for the estimation of the minimum travel–time increment $d_{\rm min}$ between the gridpoint initiating updating and the updated gridpoint. This is, of course, a very rough approximation, but is applied only locally and is secured with the minimum slowness. In addition, we shall restrict the derivation to the vicinity of the point source where the influence of the wavefront curvature on the minimum travel–time increment is probably most pronounced.

We shall consider here the local coordinates parallel with gridlines and centred at the point source. Assume 4 gridpoints

$$A=(x,y),\ B=(x+h,y),\ C=(x,y+h),\ D=(x+h,y+h)\quad , \tag{1}$$

where h is the grid spacing. Assume that the coordinates are chosen in such a way that

$$y \geq x \geq 0\quad . \tag{2}$$

If point B is selected to initiate updating, then only point A of these points has smaller travel time than B and the "refraction" updating (**a**) is started from gridline segment AB. The gridpoints to be updated are C and D. If

$$x+h < h+H \qquad \text{and} \qquad y < h+H\quad , \tag{3}$$

point B has already been updated during the initialization and placed in the queue in front of C and D. Since the minimum travel–time increment is used to avoid premature updating of C or D if placed in the queue in front of B, we shall constrain the derivation by

$$x+h \geq h+H \qquad \text{or} \qquad y \geq h+H\quad . \tag{4}$$

The travel–time increment between B and D may be limited by

$$d_0(x,y)=\left[\sqrt{(x+h)^2+(y+h)^2}-\sqrt{(x+h)^2+y^2}\right]\,u_{\rm min}\quad . \tag{5}$$

Under constraints (2) and (4), function (5) has minimum

$$d_0=\left[\sqrt{2}\,(h+H)-\sqrt{(h+H)^2+H^2}\right]\,u_{\rm min}\quad . \tag{6}$$

Under constraints (2), "refraction" updating (**a**) is applied to gridpoint C only if $x=0$. The travel–time increment between B and C may then be limited by

$$d_1(y)=\left[\sqrt{0^2+(y+h)^2}-\sqrt{(0+h)^2+y^2}\right]\,u_{\rm min}\quad . \tag{7}$$

Under constraints (4) with $x=0$, function (7) has minimum

$$d_1=\left[2h+H-\sqrt{(h+H)^2+h^2}\right]\,u_{\rm min}\quad , \tag{8}$$

which is greater than (6) and thus need not be taken into account.

The minimum travel–time increment (6) is increasing with H, and approaches its minimum value of

$$d_{\rm min}=(\sqrt{2}-1)\,h\,u_{\rm min} \tag{9}$$

for H approaching zero.

Since the difference between (9) and (6) should not substantially affect the numerical efficiency of the algorithm, and since the above considerations are, to some extent, approximate, we suggest (9) is used as the lower bound of (6), independent of H.

3 Travel–time calculation

3.1 Propagation of type (a) : "refraction"

Let us assume that Y_0 is the endpoint of gridline segment Y_0Y_1 initiating updating, nearest to the updated point Y_2, whereas Y_1 is the more distant one. For the travel–time interpolation, a local coordinate system may be introduced by the following simple transformation of a general 2-D Cartesian coordinate system connected with the grid: the origin is moved to point Y_0, and, if the gridline segment Y_0Y_1 is not parallel with the first coordinate axis, the two coordinates are exchanged. Endpoints Y_0 and Y_1 of the gridline segment initiating updating, and gridpoint Y_2 to be updated then have coordinates

$$\mathbf{x}_0 = (0,0) \ , \quad \mathbf{x}_1 = (\Delta x_1, 0) = (\pm h, 0) \ , \quad \mathbf{x}_2 = (0, \Delta x_2) = (0, \pm h) \ , \tag{10}$$

respectively. We also denote the corresponding travel times and slowness vectors in the local coordinate system

$$\tau_0 \ , \ \mathbf{p}_0 = (p_{10}, p_{20}) \ , \quad \tau_1 \ , \ \mathbf{p}_1 = (p_{11}, p_{21}) \ , \quad \tau_2 \ , \ \mathbf{p}_2 = (p_{12}, p_{22}) \ . \tag{11}$$

3.1.1 Linear slowness interpolation

Slowness is linearly interpolated inside the triangle $Y_0Y_1Y_2$, from slowness u_0 at Y_0, slowness u_1 at Y_1, and u_2 at Y_2,

$$u(x_1, x_2) = u_0 + U_1 x_1 + U_2 x_2 \quad , \tag{12}$$

with

$$\Big(U_1, U_2\Big) = \Big(\frac{u_1 - u_0}{\Delta x_1}, \frac{u_2 - u_0}{\Delta x_2}\Big) \tag{13}$$

being the slowness gradient.

3.1.2 Backprojection of the updated gridpoint

First, the backprojection $\tilde{Y}_2$ of the updated gridpoint Y_2 onto the gridline segment Y_0Y_1 initiating updating is determined; see Figure 2. The point of intersection of two straight lines given by the slowness vectors is selected as centre C of the central projection. This means that the backprojected point lies on the straight line connecting centre C and gridpoint Y_2 to be updated.

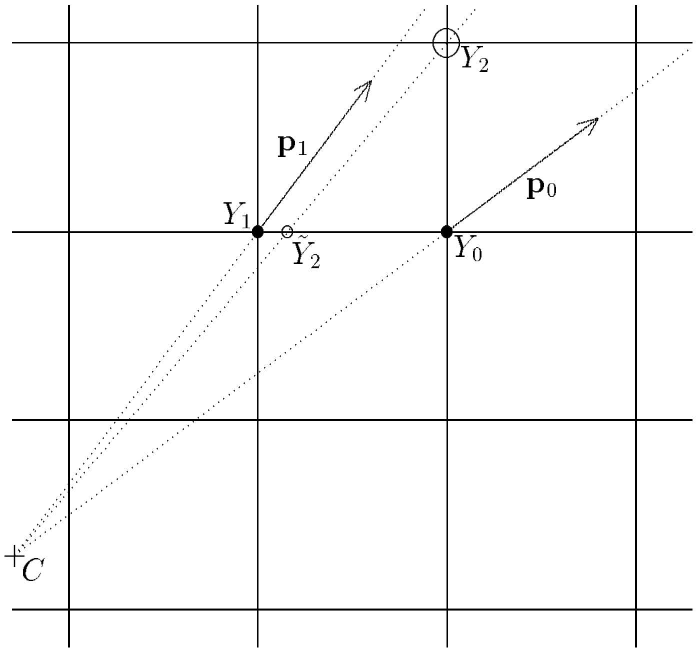

Figure 2. Y_0 and Y_1 are two end gridpoints of the gridline segment along which the travel time has already been determined and which initiate updating; Y_2 is the gridpoint to be updated if the new travel time is less than the previously determined value; C is the point of intersection of straight lines given by the slowness vectors; $\tilde{Y}_2$ is the backprojection of the gridpoint to be updated, i.e. the point at which the travel time is interpolated.

3.1.3 Cubic or quadratic travel–time interpolation

Gridpoint Y_2 cannot be updated unless

$$\frac{p_{20}}{\Delta x_2} > 0 \quad \text{and} \quad \frac{p_{21}}{\Delta x_2} > 0 \quad , \tag{14}$$

i.e., unless the wavefront propagates from segment Y_0Y_1 towards gridpoint Y_2 and not to the opposite side. For the notation refer to (10) and (11).

If inequalities (14) are in force, the projections of points Y_0 and Y_1 onto the parallel gridline through Y_2 are

$$\tilde{\mathbf{x}}_0 = \left(\tilde{x}_{10}, \Delta x_2\right) = \left(\frac{p_{10}\Delta x_2}{p_{20}}, \Delta x_2\right) , \quad \tilde{\mathbf{x}}_1 = \left(\tilde{x}_{11}, \Delta x_2\right) = \left(\Delta x_1 + \frac{p_{11}\Delta x_2}{p_{21}}, \Delta x_2\right) . \tag{15}$$

Point Y_2 can be updated if it is situated inbetween the projections,

$$\frac{\tilde{x}_{10}}{\Delta x_1} < 0 \quad \text{and} \quad 0 < \frac{\tilde{x}_{11}}{\Delta x_1} \quad . \tag{16}$$

The backprojection $\tilde{Y}_2$ of point Y_2 is then

$$\tilde{\mathbf{x}}_2 = \Big(\tilde{x}_{12}, 0\Big) = \Big(\frac{\Delta x_1 \tilde{x}_{10}}{\tilde{x}_{10} - \tilde{x}_{11}}, 0\Big) \quad . \tag{17}$$

3.1.3.1 Cubic travel–time interpolation

The travel time between points Y_0 and Y_1 may be interpolated by third–order Hermite polynomial interpolation with respect to $\tilde{x}_{12}$,

$$\tau(\tilde{x}_{12}) = (2a_0 + 1)a_1 a_1(\tau_0 - \tau_1) + \tau_1 + a_0 a_1(a_1 p_{10} + a_0 p_{11})\Delta x_1 \quad , \tag{18}$$

where

$$a_0(\tilde{x}_{12}) = \frac{\tilde{x}_{12}}{\Delta x_1} \ , \quad a_1(\tilde{x}_{12}) = a_0(\tilde{x}_{12}) - 1 \ . \tag{19}$$

If the backprojection coincides with Y_0, $a_0 = 0$, and if the backprojection coincides with Y_1, $a_1 = 0$. Taking into account that the derivatives of both a_0 and a_1 with respect to $\tilde{x}_{12}$ equal $(\Delta x_1)^{-1}$, the first and second derivatives of (18) are

$$p_1(\tilde{x}_{12}) = 6a_0 a_1(\tau_0 - \tau_1)(\Delta x_1)^{-1} + (2a_0 + a_1)a_1 p_{10} + (a_0 + 2a_1)a_0 p_{11} \tag{20}$$

and

$$T_{11}(\tilde{x}_{12}) = 6(a_0 + a_1)(\tau_0 - \tau_1)(\Delta x_1)^{-2} + 2[(a_0 + 2a_1)p_{10} + (2a_0 + a_1)p_{11}](\Delta x_1)^{-1} \ . \tag{21}$$

If there is an error δp_1 in p_{10} and p_{11}, this error is projected through equation (20) onto the new slowness–vector components p_1, with a multiplication factor of

$$q = (2a_0 + a_1)a_1 + (a_0 + 2a_1)a_0 = 1 + 6a_0 a_1 \quad . \tag{22}$$

Multiplication factor (22) is limited by inequalities $-\frac{1}{2} \leq q \leq 1$ resulting from (19). For multiplication factors q close to 1, the error δp_1 in the slowness–vector accumulates along rays, and the accumulated error is projected by means of equation (18) onto the travel time, see Section 4.1.

3.1.3.2 Quadratic travel–time approximation

The accumulation of error δp_1 in the slowness–vector may be avoided by a modification of interpolation (18). If the average slowness–vector component $\frac{1}{2}(p_{10} + p_{11})$ is replaced in (18) by the difference $(\tau_1 - \tau_0)(\Delta x_1)^{-1}$, while considering the wavefront curvature described by the difference $p_{11} - p_{10}$ of the slowness–vector components, equation (18) is turned into the quadratic approximation

$$\tau(\tilde{x}_{12}) = \tau_0 + a_0(\tau_1 - \tau_0) + \tfrac{1}{2}a_0 a_1(p_{11} - p_{10})\Delta x_1 \quad . \tag{23}$$

Taking into account that the derivatives of both a_0 and a_1 with respect to $\tilde{x}_{12}$ equal $(\Delta x_1)^{-1}$, the first and second derivatives of (23) are

$$p_1(\tilde{x}_{12}) = (\tau_1 - \tau_0)(\Delta x_1)^{-1} + \tfrac{1}{2}(a_0 + a_1)(p_{11} - p_{10}) \tag{24}$$

and

$$T_{11}(\tilde{x}_{12}) = (p_{11} - p_{10})(\Delta x_1)^{-1} \ . \tag{25}$$

Although the quadratic approximation (23) generates a local relative travel–time error of order h^2 not contained in (18), it is usually globally more stable and accurate than (18) because accumulation of error in the orientation of the slowness vector is avoided. For example, compare Figures 3b and 3c of Section 6.

3.1.4 Spherical correction

The above cubic interpolation or quadratic approximation is sufficiently accurate if the centre C of the central projection,

$$x_2^C = \frac{\Delta x_1}{\left(\frac{p_{10}}{p_{20}} - \frac{p_{11}}{p_{21}}\right)} \quad , \quad x_1^C = \frac{p_{10}}{p_{20}}\, x_2^C \quad , \tag{26}$$

is sufficiently distant from the gridline Y_0Y_1. In practice, "sufficiently distant" may mean at least N grid intervals with given N,

$$N \left| \frac{p_{10}}{p_{20}} - \frac{p_{11}}{p_{21}} \right| < 1 \quad . \tag{27}$$

The value of N affects, for instance, the accuracy in the vicinity of the point source. Although the cubic interpolation is very accurate if the point source is at a gridpoint even without this restriction, for a general source position and possibly in some other situations, the value of N should not be less than 2. On the other hand, N is unlikely to have to exceed 20 even for very accurate testing calculations. As we shall see below, large N slows down the computation, but not considerably. That is why N need not be chosen too small. The author recommends values of N from 10 to 20, believing that $N = 10$ should be sufficient for all contemporary seismological applications.

If inequality (27) is not in force, cubic interpolation or quadratic approximation of the spherical wavefront may not be sufficiently accurate. In such a case, a reference travel–time distribution along gridline segment Y_0Y_1, resembling spherical wavefronts, may be introduced in order to interpolate only the travel–time residuals with respect to the reference solution.

In accordance with the central projection employed above (see Figure 2), a simple reference travel–time distribution is introduced: the slowness vectors along gridline segment Y_0Y_1 are assumed to have the directions of the projecting straight lines passing through the centre C of the central projection. Since the length of the slowness vector equals slowness

$$u(x_1, 0) = u_0 + U_1 x_1 \tag{28}$$

linearly interpolated along the gridline, the assumption yields the travel–time derivative along the gridline,

$$\mathring{p}_1(x_1) = \frac{x_1 - x_1^C}{r(x_1)}\, u(x_1, 0) \quad , \tag{29}$$

where

$$r(x_1) = \sqrt{(x_1 - x_1^C)^2 + (x_2^C)^2} \tag{30}$$

is the distance from centre C. The reference travel time is then the integral of its derivative (29),

$$\mathring{\tau}(x_1) = \tfrac{1}{2} \left\{ r(x_1) \left[u(x_1, 0) + u(x_1^C, 0) \right] - U_1 \left[x_2^C \right]^2 \ln \left(r(x_1) + x_1 - x_1^C \right) \right\} \quad . \tag{31}$$

The second reference travel–time derivative

$$\mathring{T}_{11}(x_1) = \frac{[x_2^C]^2}{[r(x_1)]^3}\, u(x_1, 0) + \frac{x_1 - x_1^C}{r(x_1)}\, U_1 \tag{32}$$

is the result of differentiating (29).

The travel–time and first slowness–vector component residuals are

$$\tilde{\tau}_0 = \tau_0 - \mathring{\tau}(0) \ , \ \tilde{p}_{10} = 0 \ , \quad \tilde{\tau}_1 = \tau_1 - \mathring{\tau}(\Delta x_1) \ , \ \tilde{p}_{11} = 0 \ . \tag{33}$$

3.1.4.1 Spherical correction with cubic interpolation

If cubic interpolation of travel times described in Section 3.1.3.1 is chosen, travel–time residuals (33) may be interpolated by cubic interpolation (18),

$$\tilde{\tau}(\tilde{x}_{12}) = (2a_0 + 1)a_1 a_1(\tilde{\tau}_0 - \tilde{\tau}_1) + \tilde{\tau}_1 \quad , \tag{34}$$

$$\tilde{p}_1(\tilde{x}_{12}) = 6a_0 a_1(\tilde{\tau}_0 - \tilde{\tau}_1)(\Delta x_1)^{-1} \quad , \tag{35}$$

$$\tilde{T}_{11}(\tilde{x}_{12}) = 6(a_0 + a_1)(\tilde{\tau}_0 - \tilde{\tau}_1)(\Delta x_1)^{-2} \quad . \tag{36}$$

3.1.4.2 Spherical correction with linear approximation

If quadratic approximation of travel times described in Section 3.1.3.2 is chosen, the travel–time residuals (33) should be approximated by linear interpolation

$$\tilde{\tau}(\tilde{x}_{12}) = a_1(\tilde{\tau}_0 - \tilde{\tau}_1) + \tilde{\tau}_1 \quad , \tag{37}$$

$$\tilde{p}_1(\tilde{x}_{12}) = (\tilde{\tau}_0 - \tilde{\tau}_1)(\Delta x_1)^{-1} \quad , \tag{38}$$

$$\tilde{T}_{11}(\tilde{x}_{12}) = 0 \quad . \tag{39}$$

The resulting interpolated quantities at the backprojection $\tilde{Y}_2$ of the updated grid-point Y_2 are

$$\tau(\tilde{x}_{12}) = \mathring{\tau}(\tilde{x}_{12}) + \tilde{\tau}(\tilde{x}_{12}) \quad , \tag{40}$$

$$p_1(\tilde{x}_{12}) = \mathring{p}_1(\tilde{x}_{12}) + \tilde{p}_1(\tilde{x}_{12}) \quad , \tag{41}$$

and

$$T_{11}(\tilde{x}_{12}) = \mathring{T}_{11}(\tilde{x}_{12}) + \tilde{T}_{11}(\tilde{x}_{12}) \quad . \tag{42}$$

Residual quantities $\tilde{\tau}$, $\tilde{p}_1$, and $\tilde{T}_{11}$ in (40)–(42) are given by (34)–(36) or (37)–(39), respectively.

3.1.5 Slowness–vector extrapolation

We denote $\tilde{u}_2 = u(\tilde{x}_{12}, 0)$ the slowness at backprojection $\tilde{Y}_2$. If

$$(\tilde{u}_2)^2 > (p_1)^2 \quad , \tag{43}$$

which should apply to all reasonably discretized models, the second slowness component at $\tilde{Y}_2$ is

$$p_2 = \mathrm{sign}(\Delta x_2)\sqrt{(\tilde{u}_2)^2 - (p_1)^2} \quad . \tag{44}$$

The remaining second partial travel–time derivatives follow from equations

$$\tilde{u}_2 U_1 = T_{11} p_1 + T_{12} p_2 \ , \quad \tilde{u}_2 U_2 = T_{12} p_1 + T_{22} p_2 \tag{45}$$

and are given by

$$T_{12} = (\tilde{u}_2 U_1 - p_1 T_{11})(p_2)^{-1} \ , \quad T_{22} = (\tilde{u}_2 U_2 - p_1 T_{12})(p_2)^{-1} \ . \tag{46}$$

Now the slowness vector at Y_2 may be approximated by a Taylor expansion,

$$\bar{p}_{12} = p_1 - T_{11}\tilde{x}_{12} + T_{12}\Delta x_2 \ , \quad \bar{p}_{22} = p_2 - T_{12}\tilde{x}_{12} + T_{22}\Delta x_2 \ . \tag{47}$$

Finally, the slowness vector at gridpoint Y_2 is normalized,

$$p_{12} = u_2\, \bar{p}_{12} / \sqrt{(\bar{p}_{12})^2 + (\bar{p}_{22})^2} \ , \quad p_{22} = u_2\, \bar{p}_{22} / \sqrt{(\bar{p}_{12})^2 + (\bar{p}_{22})^2} \ . \tag{48}$$

3.1.6 Travel–time evaluation

Equation

$$\tau_2 = \tau + \tfrac{1}{2}\left\{-[p_1 + p_{12}]\tilde{x}_{12} + [p_2 + p_{22}]\Delta x_2\right\} \tag{49}$$

may then be used to calculate the travel time at the updated gridpoint Y_2 using the averaged slowness vectors at points $\tilde{Y}_2$ and Y_2. Equation (49) is accurate up to the second–order terms in the Taylor expansion of travel time.

3.2 Propagation of type (b) : diffractions at gridpoints

The travel time between point $\mathbf{x} = (x_1, 0)$ and $\mathbf{x}_2 = (0, \Delta x_2)$ is approximately

$$\Delta\tau = \frac{u(x_1, 0) + u_2}{2}\sqrt{[x_1]^2 + [\Delta x_2]^2} \quad . \tag{50}$$

The accuracy of (50) is very similar (although not exactly the same) as of (49). The corresponding slowness vector at Y_2 may be approximated as

$$(\bar{p}_{12}, \bar{p}_{22}) = \frac{u(x_1, 0) + u_2}{2} \frac{(-x_1, \Delta x_2)}{\sqrt{[x_1]^2 + [\Delta x_2]^2}} + \frac{1}{2}(U_1, U_2)\sqrt{[x_1]^2 + [\Delta x_2]^2} \tag{51}$$

and normalized according to (48). For propagation from Y_0 to Y_2, $x_1 = 0$ in (50) and (51), and for propagation from Y_1 to Y_2, $x_1 = \Delta x_1$ in (50) and (51).

4 Accuracy estimations

We denote the second partial derivatives of slowness u in the local coordinates U_{11}, $U_{12} = U_{21}$, and U_{22}, the third partial derivatives of travel time in the local coordinates T_{IJK}, and the vector from the backprojection $\tilde{Y}_2$ to updated point Y_2 $\mathbf{E} = (E_1, E_2)$,

$$\mathbf{E} = (-\tilde{x}_{12}, \Delta x_2) \quad , \tag{52}$$

all in the local coordinates.

4.1 Error of slowness–vector extrapolation

The error of the slowness–vector extrapolation (34) due to neglected third partial travel–time derivatives is

$$\Delta \bar{p}_I = -\tfrac{1}{2} T_{IJK} E_J E_K \tag{53}$$

per single extrapolation. By normalization (48), the error is projected onto the wavefront tangent plane,

$$\Delta p_I = \left(\delta_{IM} - \frac{E_I E_M}{|\mathbf{E}|^2} \right) \Delta \bar{p}_M \quad . \tag{54}$$

The error is then accumulated during repeated interpolations (20) with quotient q, see (22),

$$\delta p_1 = \Delta p_1 \, (1 - q)^{-1} = -\Delta p_1 \, (6 a_0 a_1)^{-1} \quad . \tag{55}$$

The relative travel–time error due to this accumulated slowness–vector error is, see (18),

$$\rho\tau_{(1)} = a_0 a_1 (a_0 + a_1) \, \delta p_1 \, \Delta x_1 \, (u |\mathbf{E}|)^{-1} = -(a_0 + a_1) \, \Delta p_1 \, \Delta x_1 \, (6 u |\mathbf{E}|)^{-1} \quad , \tag{56}$$

which may be expressed, using (19), (53) and (54), as

$$\rho\tau_{(1)} = \frac{2\tilde{x}_{12} - \Delta x_1}{12 \, u} \left(\delta_{1M} - \frac{E_1 E_M}{|\mathbf{E}|^2} \right) \frac{T_{MJK} E_J E_K}{|\mathbf{E}|} \quad . \tag{57}$$

4.2 Error of quadratic travel–time approximation

The error of quadratic travel–time approximation (23) due to a neglected third partial travel–time derivative is

$$\rho\tau_{(2)} = -\frac{T_{111} \, \tilde{x}_{12} (\tilde{x}_{12} - \Delta x_1)(2\tilde{x}_{12} - \Delta x_1)}{12 \, u \, |\mathbf{E}|} \quad . \tag{58}$$

4.3 Error of linear slowness interpolation

The error of linear slowness interpolation (12) at point $\tilde{Y}_2$ is

$$\delta \tilde{u}_2 = \tfrac{1}{2} U_{11} \tilde{x}_{12} (\Delta x_1 - \tilde{x}_{12}) \quad . \tag{59}$$

This slowness error introduces the additional relative error of

$$\rho\tau_{(3)} = \frac{1}{4} \frac{U_{11}}{u} \tilde{x}_{12} (\Delta x_1 - \tilde{x}_{12}) \tag{60}$$

in travel–time approximation (49).

4.4 Error of travel–time evaluation

The relative error of travel–time approximation (49) is

$$\rho\tau_{(4)} = \frac{T_{IJK}E_I E_J E_K}{12u|\mathbf{E}|} = \frac{|\mathbf{E}|^2}{12u^4}\, T_{IJK}\, p_I\, p_J\, p_K \quad . \tag{61}$$

Differentiating the eikonal equation, we arrive at

$$T_{IJK}\, p_I\, p_J\, p_K = u\, p_J\, U_{JK}\, p_K + p_J\, U_J U_K\, p_K - u^2 U_M U_M \quad . \tag{62}$$

Equation (61) may then also be expressed in the equivalent form of

$$\rho\tau_{(4)} = \frac{1}{12u^2} E_J\,(uU_{JK} + U_J U_K - U_M U_M \delta_{JK})\, E_K \quad . \tag{63}$$

4.5 Estimation of the total relative travel–time error

We assume that the quadratic travel–time approximation of Section 3.1.3.2 is used, and error (57) need not be considered. The extreme value

$$\rho\tau_{(2)\mathrm{MAX}} \approx -\frac{T_{111}}{12\,u}\frac{(\Delta x_1)^2}{10.6} \tag{64}$$

of error (58), generated for $\tilde{x}_{12} = 0.206\Delta x_1$, is smaller than 14% of the extreme value of term

$$\frac{T_{111}E_1E_1E_1}{12u|\mathbf{E}|} \tag{65}$$

appearing as a part of (61). This prompts us to neglect error (58) in comparison with error (61), and to consider errors (60) and (63) only.

Taking into account that

$$\Delta x_1 = h\,\mathrm{sign}(\tilde{x}_{12}) \quad , \tag{66}$$

see (16) and (17), the total relative error

$$\rho\tau = \rho\tau_{(3)} + \rho\tau_{(4)} \tag{67}$$

may be expressed in the form of

$$\rho\tau = \frac{1}{12u^2}\left[(-2uU_{11} - U_2U_2)|\tilde{x}_{12}|^2 \right.$$
$$\left. +[3uU_{11} - 2(uU_{12} + U_1U_2)\,\mathrm{sign}(\Delta x_1 \Delta x_2)]|\tilde{x}_{12}|\, h + (uU_{22} - U_1U_1)h^2\right] \ . \tag{68}$$

In interval $|\tilde{x}_{12}| \in < 0, h >$, function $\rho\tau = \rho\tau(|\tilde{x}_{12}|)$ has 2 to 3 local extrema,

$$\rho\tau(0) = \frac{h^2}{12u^2}[uU_{22} - U_1U_1] \quad , \tag{69}$$

$$\rho\tau(h) = \frac{h^2}{12u^2}\left[uU_{11} - U_2U_2 - 2(uU_{12} + U_1U_2)\,\mathrm{sign}(\Delta x_1 \Delta x_2) + uU_{22} - U_1U_1\right] \ , \quad (70)$$

and if

$$|\tilde{x}_{12}| = \frac{3uU_{11} - 2(uU_{12} + U_1U_2)\,\mathrm{sign}(\Delta x_1 \Delta x_2)}{2(2uU_{11} + U_2U_2)}\ h \quad (71)$$

belongs to interval $|\tilde{x}_{12}| \in <0, h>$, also

$$\rho\tau(|\tilde{x}_{12}|) = \frac{h^2}{12u^2}\left\{\frac{[3uU_{11} - 2(uU_{12} + U_1U_2)\,\mathrm{sign}(\Delta x_1 \Delta x_2)]^2}{4(2uU_{11} + U_2U_2)} + uU_{22} - U_1U_1\right\}$$

$$= \frac{h^2}{12u^2}\left\{(2uU_{11} + U_2U_2)\frac{|\tilde{x}_{12}|^2}{h^2} + uU_{22} - U_1U_1\right\} \quad . \quad (72)$$

In 2-D, the global Cartesian coordinates may be either shifted local coordinates (x_1, x_2), or shifted exchanged local coordinates (x_2, x_1), see Section 3.1. Equation (68) for the relative travel–time error may then be expressed in global Cartesian coordinates: for $|p_1| \le |p_2|$,

$$\rho\tau = \frac{h^2}{12u^2}\left[(-2uU_{11} - U_2U_2)\left|\frac{p_1}{p_2}\right|^2\right.$$

$$\left. + [3uU_{11} + 2(uU_{12} + U_1U_2)\,\mathrm{sign}(p_1p_2)]\left|\frac{p_1}{p_2}\right| + (uU_{22} - U_1U_1)\right] \quad , \quad (73)$$

and for $|p_2| \le |p_1|$,

$$\rho\tau = \frac{h^2}{12u^2}\left[(-2uU_{22} - U_1U_1)\left|\frac{p_2}{p_1}\right|^2\right.$$

$$\left. + [3uU_{22} + 2(uU_{12} + U_1U_2)\,\mathrm{sign}(p_1p_2)]\left|\frac{p_2}{p_1}\right| + (uU_{11} - U_2U_2)\right] \quad . \quad (74)$$

where the second partial slowness derivatives are considered, unlike before, in global Cartesian coordinates.

5 Comparison of the accuracy with first–order methods of grid travel–time tracing and network ray tracing

5.1 Comparison of the accuracy with network shortest–path ray tracing

We denote by U_+ the most positive and by U_- the most negative eigenvalue of matrix

$$uU_{JK} - \tfrac{1}{2}U_J U_K + \tfrac{1}{2}U_M U_M \delta_{JK} \quad . \tag{75}$$

The maximum relative travel–time error of the network shortest–path ray tracing according to Klimeš and Kvasnička (1994) in a smooth 2-D medium is then

$$\rho\tau_{\mathrm{NET}} \approx \sqrt{\frac{h^2}{24u^2}\max(U_+, \tfrac{1}{2}|U_-|)} \quad . \tag{76}$$

Comparing equations (75) and (76) with equations (63), (73), and (74), the relation between relative errors of grid travel–time tracing of the second order and network shortest–path ray tracing may be estimated very roughly as

$$|\rho\tau| \approx 2(\rho\tau_{\mathrm{NET}})^2 \quad . \tag{77}$$

5.2 Comparison of the accuracy with first–order grid travel–time tracing

Let us now estimate the relative travel–time error of the first–order grid travel–time tracing method by Podvin and Lecomte (1991). Assume the travel times $\tau_\pm$ at 2 gridpoints with coordinates $(\pm\frac{1}{2}h, -\frac{1}{2}h)$ to be known, and travel time τ at gridpoint with coordinates $(\frac{1}{2}h, \frac{1}{2}h)$ to be calculated. The Taylor expansions of the travel times from point $(0,0)$ are

$$\tau_\pm = T \pm p_1\tfrac{1}{2}h - p_2\tfrac{1}{2}h + \tfrac{1}{2}(T_{11}+T_{22})(\tfrac{1}{2}h)^2 \mp T_{12}(\tfrac{1}{2}h)^2 \quad , \tag{78}$$

$$\tau = T + p_1\tfrac{1}{2}h + p_2\tfrac{1}{2}h + \tfrac{1}{2}(T_{11}+T_{22})(\tfrac{1}{2}h)^2 + T_{12}(\tfrac{1}{2}h)^2 \quad . \tag{79}$$

The calculated travel time at point $(\frac{1}{2}h, \frac{1}{2}h)$ is

$$\begin{aligned}\tau_{\mathrm{FIRST}} &= \tau_+ + h\sqrt{u^2 - \left(\frac{\tau_+ - \tau_-}{h}\right)^2} = \tau_+ + h\sqrt{u^2 - (p_1 - T_{12}\tfrac{1}{2}h)^2} \\ &\approx \tau_+ + h\sqrt{(p_2)^2 + p_1 T_{12} h} \approx \tau_+ + h\,(p_2 + \tfrac{1}{2}\frac{p_1}{p_2}T_{12}h) \quad . \end{aligned} \tag{80}$$

Here $u = \sqrt{(p_1)^2 + (p_2)^2}$ is the slowness at the centre $(0,0)$ of the cell. The absolute error is then

$$\delta\tau_{\mathrm{FIRST}} = \tau_{\mathrm{FIRST}} - \tau \approx -p_2 h - 2T_{12}(\tfrac{1}{2}h)^2 + p_2 h + \tfrac{1}{2}\frac{p_1}{p_2}T_{12}h^2 = -\tfrac{1}{2}(1 - \frac{p_1}{p_2})T_{12}h^2 \ . \tag{81}$$

The corresponding relative travel–time error is

$$\rho\tau_{\mathrm{FIRST}} = \delta\tau_{\mathrm{FIRST}}\frac{p_2}{u^2 h} \approx -\frac{h}{2u^2}(p_2 - p_1)T_{12} \quad . \tag{82}$$

This result is valid in local coordinates chosen in such a way that both the local slowness vector components p_1 and p_2 are positive and $p_1 \leq p_2$. For instance, for propagation in the direction of the x_2 axis, $p_2 - p_1 = u$ and $T_{12} = U_1$. The mixed second partial travel–time derivative T_{12} may also be expressed using wavefront curvature $K = M/u$ as

$$T_{12} = \frac{(p_1)^3}{u^3} U_2 + \frac{(p_2)^3}{u^3} U_1 - \frac{p_1 p_2}{u} K \quad . \tag{83}$$

For instance, in the vicinity of a point source, the main contribution to derivative (83) is due to the wavefront curvature $K \approx \frac{1}{r}$. Then

$$T_{12} \approx -\frac{p_1 p_2}{u} K \approx -\frac{p_1 p_2}{ur} \tag{84}$$

and the contribution to (82) due to the wavefront curvature is

$$\rho\tau_{\mathrm{SOURCE}} \approx \frac{h\ p_1 p_2 (p_2 - p_1)}{2u^3 r} \quad . \tag{85}$$

Contribution (85) to relative error (82) has maximum

$$\rho\tau_{\mathrm{SOURCE}} \approx \frac{h}{6\sqrt{3}r} \tag{86}$$

in the direction of

$$p_1/u = \sqrt{\frac{5}{12}} - \sqrt{\frac{1}{12}} \quad , \qquad p_2/u = \sqrt{\frac{5}{12}} + \sqrt{\frac{1}{12}} \quad . \tag{87}$$

In regions where the wavefront curvature in (83) is negligible, error (82) may be roughly twice larger than that of the network shortest–path ray tracing, and the relation between the relative errors of grid travel–time tracing of the second and first orders may be estimated very roughly as

$$\rho\tau \approx \tfrac{1}{2} (\rho\tau_{\mathrm{FIRST}})^2 \quad . \tag{88}$$

6 Numerical examples: Constant velocity gradient models

6.1 Constant vertical velocity gradient, velocity contrast 1:3

In the 1-D constant velocity gradient model, the velocity increases linearly with depth. The velocity ratio between top and bottom is 1:3, velocity gradient is $2\,\mathrm{s}^{-1}$. The source is situated at the left–hand top corner of a vertical square in which the first–arrival travel times are calculated. The model has been used by Podvin and Lecomte (1991) to study the accuracy of their first–order grid travel–time tracing method, and then by Klimeš and Kvasnička (1994) to demonstrate the accuracy of network shortest–path ray tracing.

The 2-D grid of 201×201 nodes (200×200 cells) was chosen to cover the square, as in the two papers referred to above. The second–order grid travel–time tracing method proposed in this paper has been compared with the results of the first–order method by Podvin and Lecomte (1991). The analytical solution was subtracted from the first–arrival travel times calculated at the gridpoints by both the methods to yield the absolute travel–time errors.

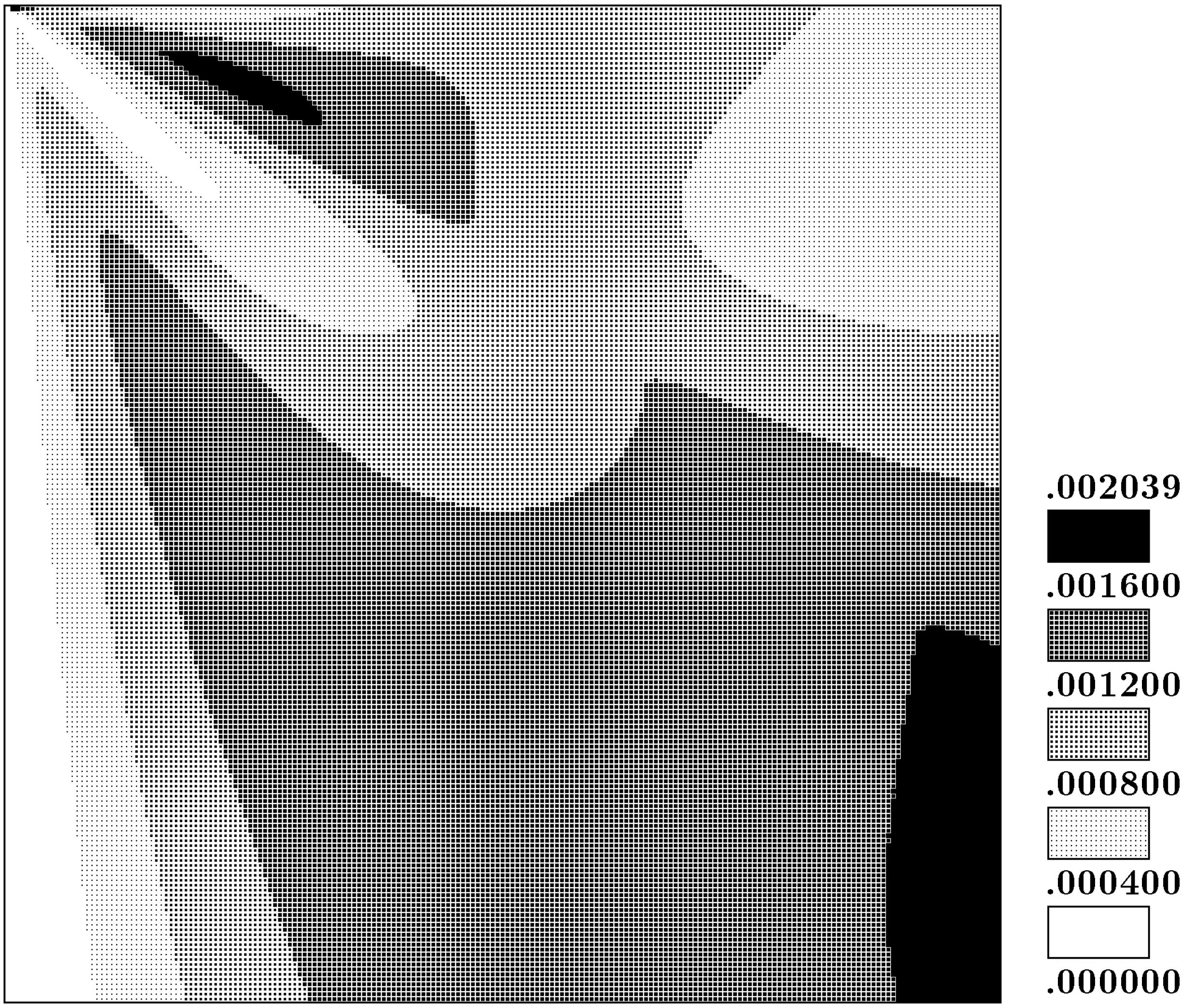

Figure 3a. Constant velocity gradient model. Travel–time errors of the first–order grid travel–time tracing method proposed by Podvin and Lecomte (1991). The absolute errors of the first–arrival travel time are scaled in seconds. Program `TIME_2D` revision `6 May 1993`.

For comparison, the absolute travel–time errors of the first–order method proposed by Podvin and Lecomte (1991) are shown in Figure 3a. Let us remark that the errors of first–order network shortest–path ray tracing by Klimeš and Kvasnička (1994) are four times smaller, see Klimeš (1996).

The absolute travel–time errors of the second–order grid travel–time tracing methods proposed in this paper are shown in Figures 3b and 3c. The two methods differ in approach to the travel–time interpolation between adjacent gridpoints. Figure 3b corresponds to the cubic travel–time interpolation between adjacent gridpoints, described in Sections 3.1.3.1 and 3.1.4.1. Figure 3c corresponds to the quadratic approximation of the travel time between adjacent gridpoints, described in Sections 3.1.3.2 and 3.1.4.2. The latter approach is now preferred by the author because of the probably better stability achieved by eliminating the accumulating differences between calculated slowness vectors and derivatives of the calculated travel time.

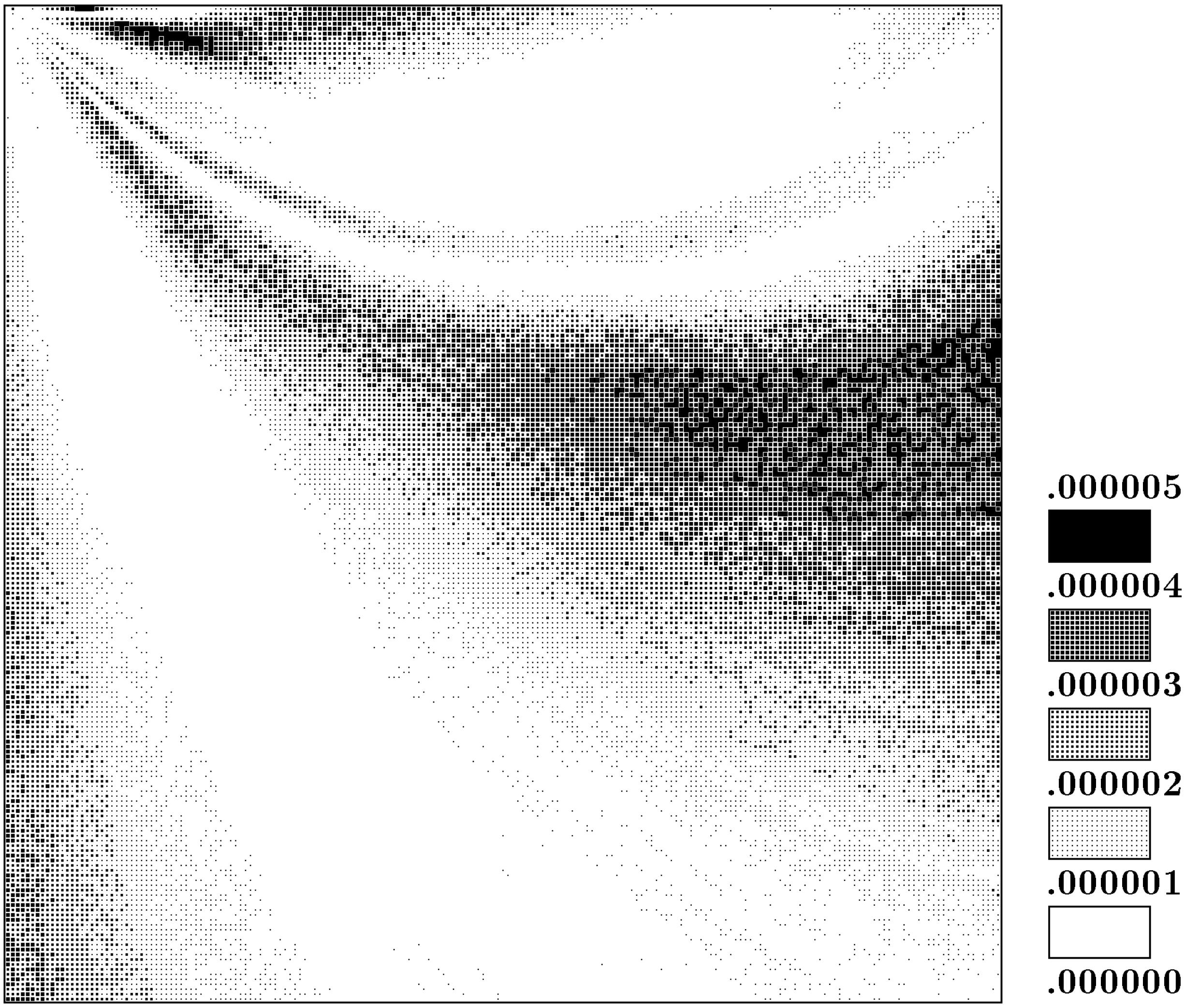

Figure 3b. Constant velocity gradient model. Travel–time errors of the second–order grid travel–time tracing according to this paper, with cubic travel–time interpolation along gridlines. The errors are scaled in seconds. Note that the error distribution has a somewhat random nature because the rounding errors are of the order of 0.000001 s, and the numerical accuracy of evaluating the reference analytical travel times is, at some gridpoints, even worse. Program `TTT-2D` version `0.06`.

Note that the errors in Figures 3b and 3c contain a somewhat random component due to rounding errors: both the numerically traced and analytical travel times have been rounded to 6 decimal places before subtracting. Moreover, the numerical errors of evaluating analytical travel times may reach at some points an absolute error of 0.000002 s or even more. For example, the error at the second gridpoint of the top row in Figures 3b and 3c is due to the analytical solution; grid travel–time tracing is much more accurate there.

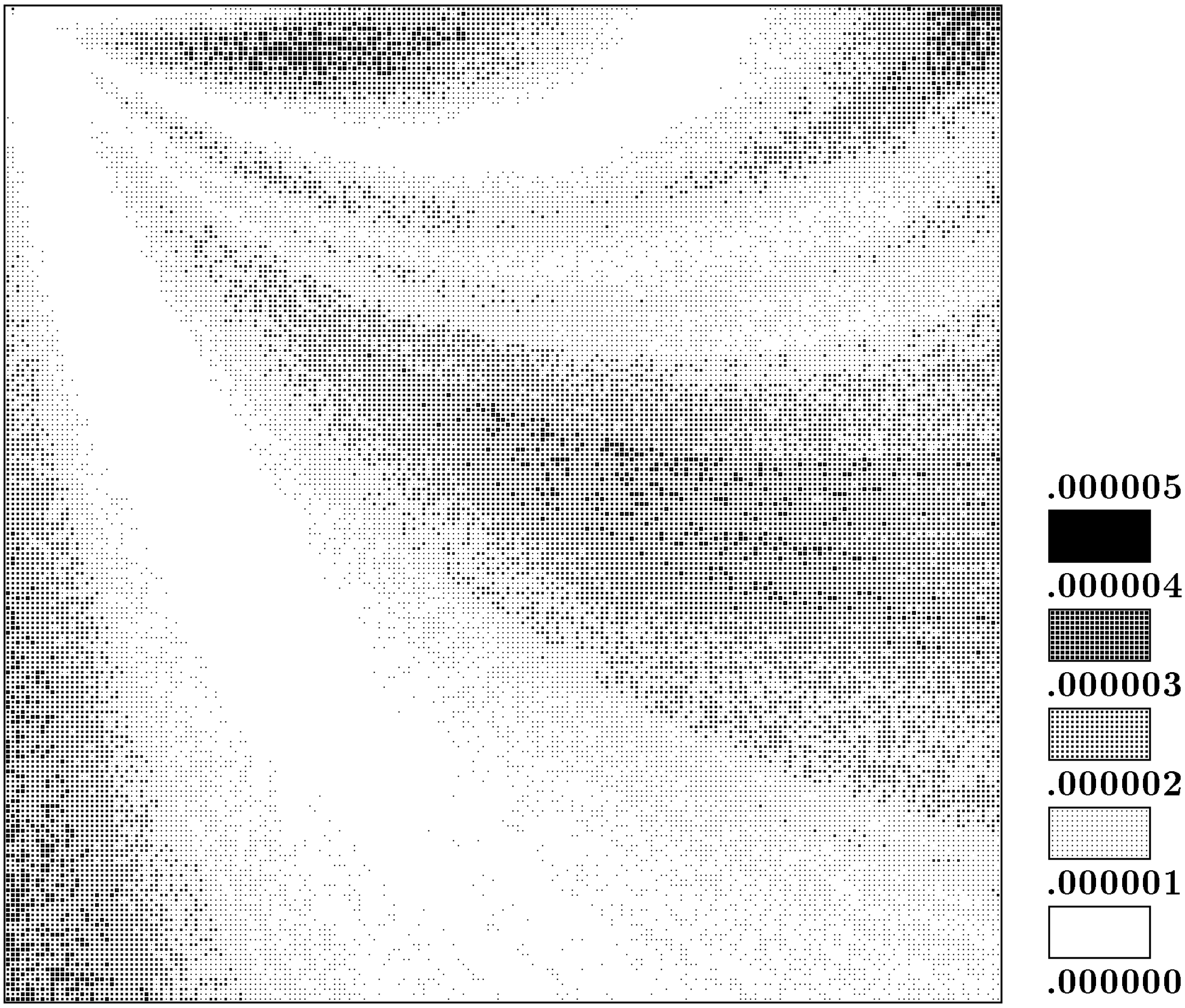

Figure 3c. Constant velocity gradient model. Travel–time errors of the second–order grid travel–time tracing according to this paper, with quadratic travel–time approximation along gridlines. The errors are scaled in seconds. Note that the error distribution has a somewhat random nature because the rounding errors are of the order of 0.000001 s, and the numerical accuracy of evaluating the reference analytical travel times is, at some gridpoints, even worse. Program `TTT-2D` version `0.07`.

6.2 Constant vertical velocity gradient, velocity contrast 1:1.25

The velocity ratio between top and bottom is 1:1.25, that corresponds to the uppermost $\frac{1}{8}$ of the previous model. The constant vertical velocity gradient is $\frac{1}{3}\,\mathrm{s}^{-1}$, which corresponds to 6 times greater travel times than in the previous model at the depth corresponding to the same velocity contrast. Horizontal dimension of the rectangle in which the first–arrival travel times are calculated is twice its height. The source is situated in the centre of the top side. The model has been used by Van Trier and Symes (1991) for comparison with Vidale (1988).

The 2-D grid of 301×151 nodes (300×150 cells) was chosen to cover the rectangle, as in the paper by Van Trier and Symes (1991). The second–order grid travel–time tracing method proposed in this paper has been compared with the results of the method implemented by Van Trier and Symes (1991) according to Vidale (1988) without the local spherical correction, with the method of Van Trier and Symes (1991), and with the first–order method by Klimeš and Kvasnička (1994). The analytical solution was subtracted from the first–arrival travel times calculated along the bottom of the model to yield the absolute travel–time errors shown in Figure 4.

⟶

Figure 4 (right). Absolute travel–time errors along the bottom of the model with constant vertical velocity gradient, described by Van Trier and Symes (1991). **(a)** The *dashed line* represents the errors of the method proposed by Vidale (1988) but without the local spherical correction, the *solid line* denotes the errors of the method by Van Trier and Symes (1991). Reprinted from Van Trier and Symes (1991). **(b)** Errors of first–order network ray tracing by Klimeš and Kvasnička (1994). Program `NET` version `2.00`. **(c)** Errors of the second–order grid travel–time tracing according to this paper, with quadratic travel–time approximation along gridlines. Note that the random component of the error distribution, conspicuous because of the scale 100 times enlarged with respect to (a) and (b), is caused by rounding errors in single precision reals. Program `TTT-2D` version `0.07`.

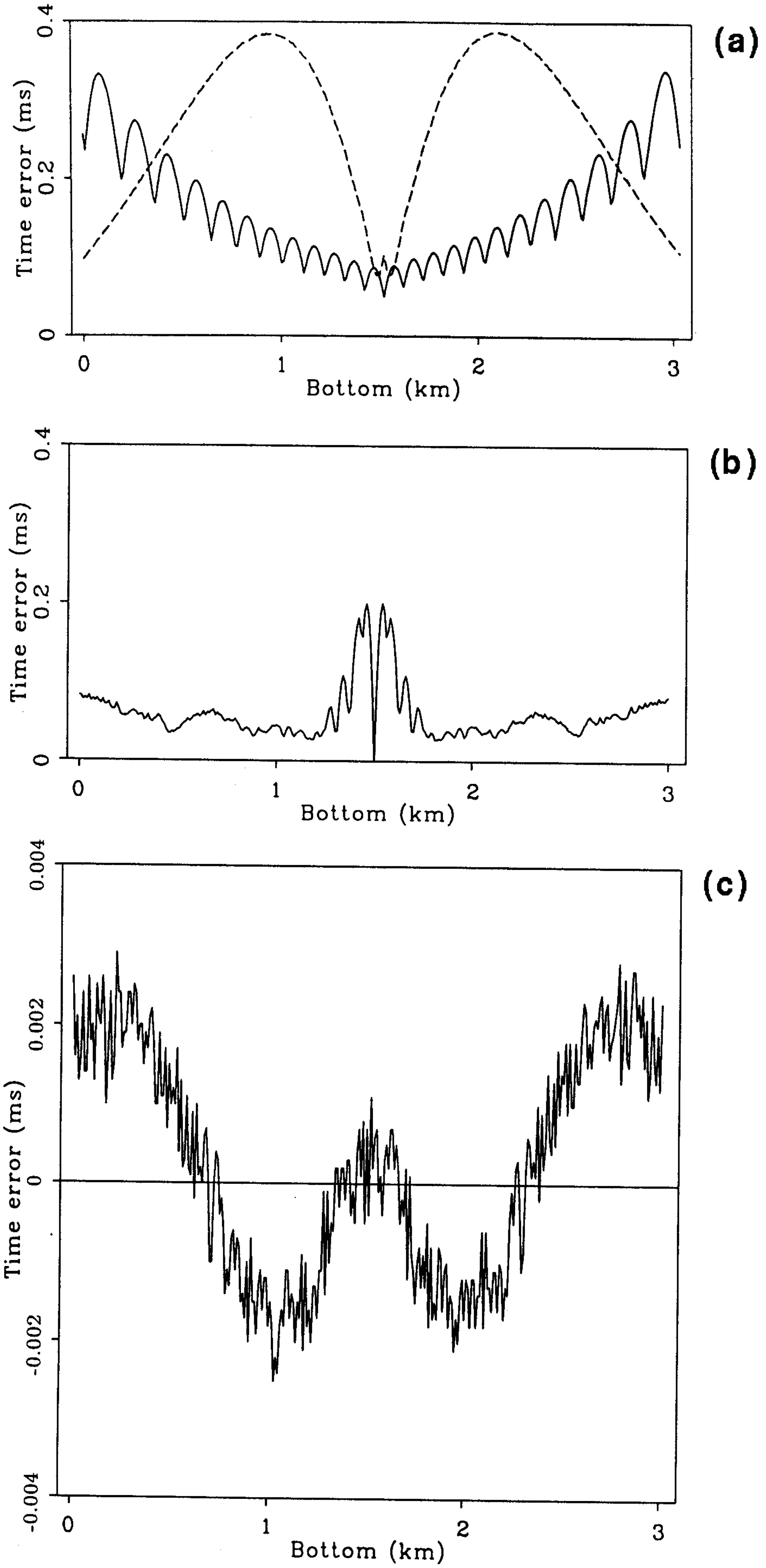
(a)
Time error (ms)
0
0.2
0.4
Bottom (km)
0
1
2
3
(b)
Time error (ms)
0
0.2
0.4
Bottom (km)
0
1
2
3
(c)
Time error (ms)
-0.004
-0.002
0
0.002
0.004
Bottom (km)
0
1
2
3

6.3 Constant slant velocity gradient

The source is situated in the centre of the top side of a vertical square in which the first–arrival travel times are calculated. The velocity ratio between the left-hand and right–hand top corners is 1:2.2, the velocity ratio between the top and bottom left–hand corners is 1:1.8. Velocity gradient is $1.5\,\mathrm{s}^{-1}$ horizontally and $1\,\mathrm{s}^{-1}$ vertically. The model has been used by Pusey and Vidale (1991) for comparison with methods proposed by Vidale (1988) and Van Trier and Symes (1991).

First, the 2-D grid of 41×41 nodes (40×40 cells) was chosen to cover the square, and the absolute errors of the second–order grid travel–time tracing method proposed in this paper has been compared with the results calculated by Pusey and Vidale (1991) on the rectangular grid of the same density using the method of Vidale (1988). According to the author's estimation, Vidale's method is also of the second order and also includes the local spherical correction. The analytical solution was subtracted from the first–arrival travel times calculated along the bottom of the model to yield the absolute travel–time errors overlaid in Figure 5 with the errors reprinted from the paper by Pusey and Vidale (1991).

Second, the 2-D grid of 101×101 nodes (100×100 cells) was chosen to cover the square, and the absolute errors of the second–order grid travel–time tracing method proposed in this paper has been compared with the results of the second–order method proposed by Pusey and Vidale (1991). The average density of gridpoints corresponds approximately to Pusey and Vidale (1991), who used in polar coordinates an angular step of 1° and a radial step corresponding to 80 intervals per a model side. The analytical solution was subtracted from the first–arrival travel times, calculated along the bottom of the model, to yield the absolute travel–time errors overlaid in Figure 6 with the errors reprinted from the paper by Pusey and Vidale (1991).

Since the method proposed in this paper is of the second–order accuracy, its errors in Figure 6 should be approximately $2.5^2 = 6.25$ times smaller than in Figure 5.

7 Structural interfaces

The above algorithm should not be used, without modification, at structural interfaces of the first order for two reasons at least:

(α) The method is proposed for a smooth medium with heterogeneities sufficiently larger than the grid interval, and is unstable in the presence of considerable slowness (or velocity) contrasts.

(β) The travel–time error due to the structural interfaces is of the order of h, which is inadequate to a method of second–order accuracy.

Thus, in addition to gridded slownesses (or velocities), information on the positions and slopes of structural interfaces must also be available for the grid travel–time tracing program. The algorithm then has to be extended to take the Snell law into account at the interfaces.

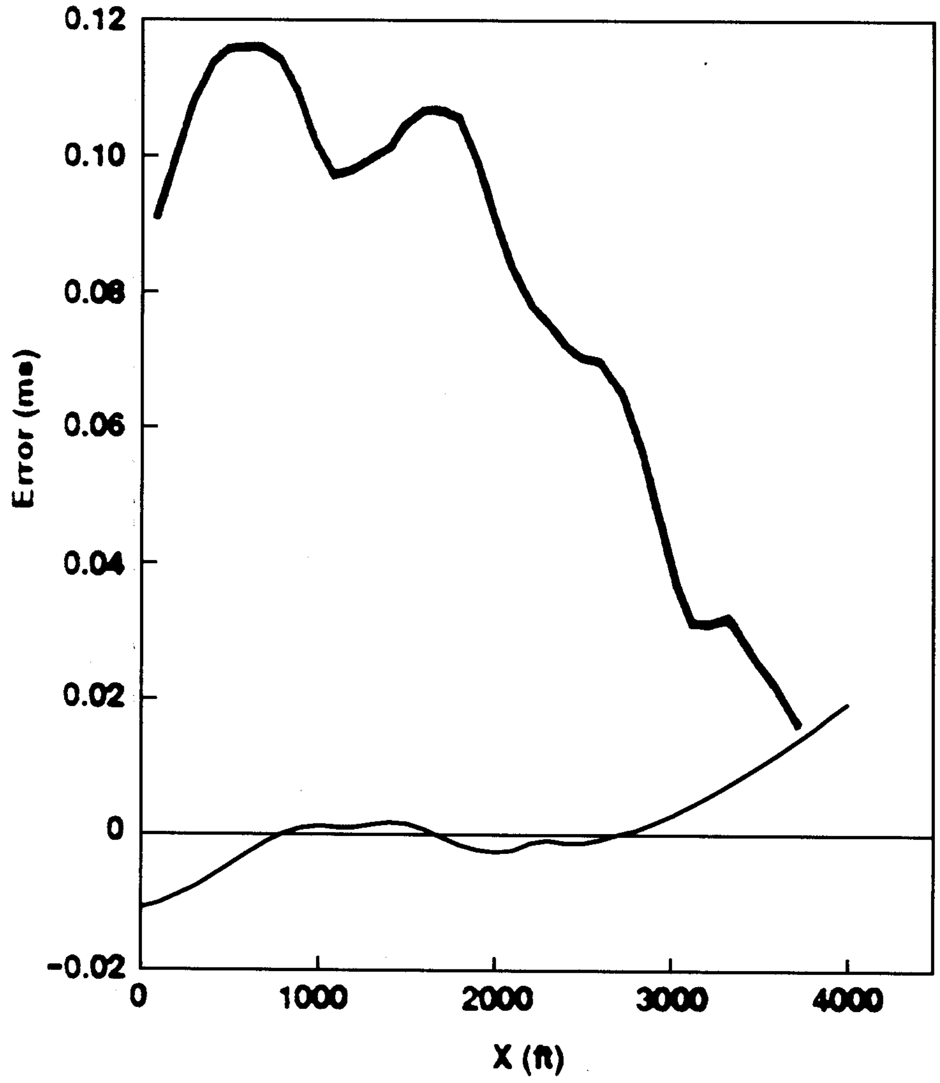

Figure 5. Absolute travel–time errors along the bottom of the model with constant slant velocity gradient, described by Pusey and Vidale (1991). Discretization 40 × 40 cells. The *bold line* represents the errors of the second–order method of Vidale (1988) with the local spherical correction, reprinted from Pusey and Vidale (1991). The *thin line* denotes the errors of the second–order method according to this paper, with quadratic travel–time approximation along gridlines (program `TTT-2D` version `0.07`).

8 Conclusions

The proposed method of grid travel–time tracing appears very promising for all practical requirements as to the accuracy and speed of the first–arrival travel–time calculation. Its accuracy is about the square of the accuracy of the contemporary first–order methods. For example, if the relative travel–time error of a first–order method is of the order of 1%, the error of the proposed second–order method should be of the order of 0.01%.

In addition to the calculated first–arrival travel times, the algorithm also enables their errors to be approximately evaluated in order to check the accuracy of the calculation.

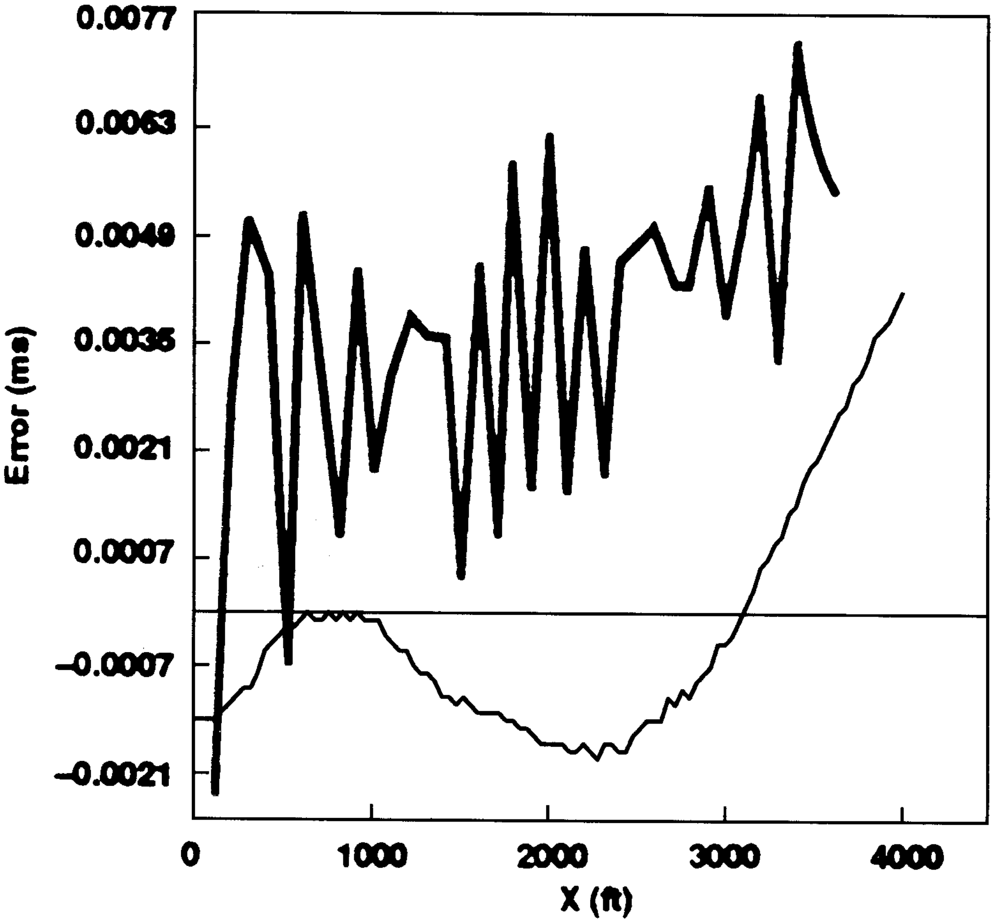

Figure 6. Absolute travel–time errors along the bottom of the model with constant slant velocity gradient, described by Pusey and Vidale (1991). The *bold line* represents the errors of the second–order method by Pusey and Vidale (1991) reprinted from their paper. The *thin line* denotes the errors of the second–order method according to this paper, with quadratic travel–time approximation along gridlines (program `TTT-2D` version `0.07`, discretization 100×100 cells).

In order to be generally applicable, the proposed algorithm has to be *extended* to *3-D*, and to *block models with curved structural interfaces* of the first order.

The method may be supplemented with an a posteriori *ray tracer*. The ray tracer may take advantage of the slowness vectors determined by the algorithm.

The accuracy of the first–order method by Podvin and Lecomte (1991) in 2-D smooth models is estimated in Section 5.2, equation (82).

Acknowledgements

The author is indebted to Vlastislav Červený, Joe Dellinger and to the anonymous reviewer for many suggestions of improving the manuscript, to Pascal Podvin for providing the `TIME_2D` program for comparison, and also to Michal Kvasnička who used it to calculate travel times for Figure 3a.

The research has been supported by the Grant Agency of the Charles University under Contract 8/94, by the Grant Agency of the Czech Republic under Contract 205/95/1465, by the Grant Agency of the Academy of Sciences of the Czech Republic under Contract 346110, by the European Commission within the framework of the JOULE II Project "Integrated Structural Imaging of Seismic Data", and by the Institut Français du Pétrole, the Shell Research B.V., the Japan National Oil Corporation, and the Elf Geoscience Research Centre within the consortium project "Seismic Waves in Complex 3-D Structures".

References

Klimeš, L. and Kvasnička, M. (1994): 3-D network ray tracing. Geophys. J. int., **116**, 726–738.

Klimeš, L. (1996): Travel–time calculation in heterogeneous 3-D structures. J. seism. Explor., submitted.

Moser, T-J. (1989): Efficient seismic ray tracing using graph theory. Expanded Abstracts of 59th Annual Int. SEG Meeting (Dallas), pp. 1106–1108, Soc. Exploration Geophysicists, Tulsa.

Moser, T-J. (1991): Shortest path calculation of seismic rays. Geophysics, **56**, 59–67.

Nakanishi, I. and Yamaguchi, K. (1986): A numerical experiment on nonlinear image reconstruction from first–arrival times for two–dimensional island arc structure. J. Phys. Earth, **34**, 195–201.

Podvin, P. and Lecomte, I. (1991): Finite difference computation of traveltimes in very contrasted velocity models: a massively parallel approach and its associated tools. Geophys. J. int., **105**, 271–284.

Pusey, L.C. and Vidale, J.E. (1991): Accurate finite–difference calculation of WKBJ traveltimes and amplitudes. Expanded Abstracts of 61st Annual Int. SEG Meeting (Houston), pp. 1513–1516, Soc. Exploration Geophysicists, Tulsa.

Qin, F., Luo, Y., Olsen, K.B. and Schuster, G.T. (1990): Solution of the eikonal equation by a finite–difference method. Expanded Abstracts of 60th Annual Int. SEG Meeting (San Francisco), pp. 1004–1007, Soc. Exploration Geophysicists, Tulsa.

Qin, F., Luo, Y., Olsen, K.B., Cai, W. and Schuster, G.T. (1992): Finite–difference solution of the eikonal equation along expanding wavefront. Geophysics, **57**, 478–487.

Saito, H. (1989): Traveltimes and raypaths of first arrival seismic waves: computation method based on Huygens' principle. Expanded Abstracts of 59th Annual Int. SEG Meeting (Dallas), pp. 244–247, Soc. Exploration Geophysicists, Tulsa.

Saito, H. (1990): 3-D ray–tracing method based on Huygens' principle. Expanded Abstracts of 60th Annual Int. SEG Meeting (San Francisco), pp. 1024–1027, Soc. Exploration Geophysicists, Tulsa.

Van Trier, J. and Symes, W.W. (1990): Upwind finite–difference calculation of seismic traveltimes. Expanded Abstracts of 60th Annual Int. SEG Meeting (San Francisco),

pp. 1000–1003, Soc. Exploration Geophysicists, Tulsa.
Van Trier, J. and Symes, W.W. (1991): Upwind finite–difference calculation of traveltimes. Geophysics, **56**, 812–821.
Vidale, J.E. (1988): Finite–difference calculation of travel times. Bull. seismol. Soc. Am., **78**, 2062–2076.
Vinje, V., Iversen, E. and Gjøystdal, H. (1993): Traveltime and amplitude estimation using wavefront construction. Geophysics, **58**, 1157–1166.